

# Recent results on $J/\psi$ , $\psi(2S)$ and $\Upsilon$ production at CDF

Robert Cropp<sup>†</sup>

Department of Physics, University of Toronto, Toronto, Canada, M5S 1A7

<sup>†</sup>For the CDF Collaboration

E-mail: rjcropp@physics.utoronto.ca

## Abstract

CDF has obtained new results on quarkonium production in  $p\bar{p}$  collisions at  $\sqrt{s} = 1.8$  TeV. We report on measurements of  $\Upsilon$  meson production,  $\Upsilon(1S)$  production from  $\chi_b$  feeddown, and the production polarization of  $\Upsilon(1S)$ ,  $J/\psi$  and  $\psi(2S)$  mesons.

## 1. Introduction

Heavy quarkonium production provides an opportunity to study QCD, both in its perturbative and nonperturbative regimes. Several analyses of quarkonia production have previously been performed by CDF using a subset of the Run I dataset. Differential cross sections for the production of  $J/\psi$ ,  $\psi(2S)$  and  $\Upsilon$  mesons were measured [1, 2]. The  $\psi$  charmonia produced in  $B$ -hadron decays were separated from the prompt (zero-lifetime) charmonia using vertex displacement. In addition, the contribution of  $\chi_c$  feeddown to prompt  $J/\psi$  production was measured [3]. It was found that the cross sections for direct  $J/\psi$  and  $\psi(2S)$  production (i.e. not from feeddown) were significantly higher than predicted by the Color Singlet Model [4], by a factor of approximately 50. This result stimulated the inclusion of color-octet  $c\bar{c}$  states in theoretical calculations of quarkonium production [5].

In this paper we present more recent studies of quarkonia production at CDF. These include new  $\Upsilon$  cross section measurements, the observation of  $\chi_b \rightarrow \Upsilon(1S)\gamma$  feeddown, and measurements of  $J/\psi$ ,  $\psi(2S)$  and  $\Upsilon(1S)$  production polarization.

The dataset used for these analyses consists of approximately  $110 \text{ pb}^{-1}$  of  $p\bar{p}$  collisions recorded during Run I of the Tevatron in 1992-95.  $J/\psi$ ,  $\psi(2S)$  and  $\Upsilon$  candidates are all recorded in their decay mode to  $\mu^+\mu^-$ , using a three-level dimuon trigger. Muons in the central pseudorapidity region ( $|\eta| < \sim 0.6$ ) are used. Muon candidates consist of tracks in the central tracking chamber matched to hits in muon chambers, located outside the calorimeter. Precise vertexing is performed by the silicon vertex detector (SVX), which measures track impact parameters with an asymptotic resolution

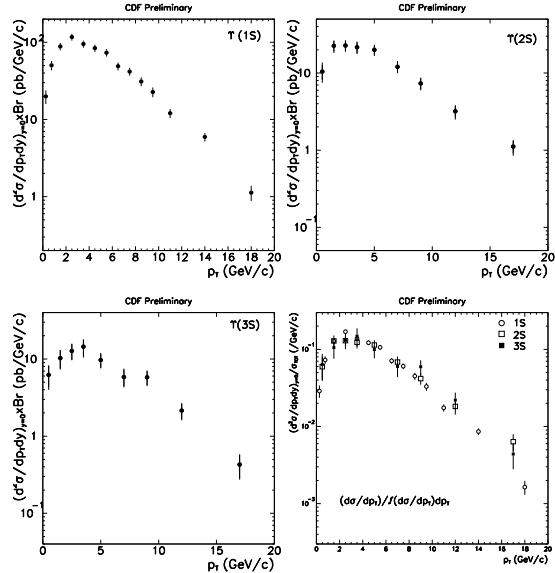


**Figure 1.** Production cross section times dimuon branching ratio for  $\Upsilon(1S)$ ,  $\Upsilon(2S)$  and  $\Upsilon(3S)$ , and a comparison of their shapes.

of  $13 \mu\text{m}$ . Photon candidates consist of energy deposits in the central electromagnetic calorimeter, matched to clusters in strip chambers embedded in the calorimeter.

## 2. Production $d\sigma/dP_T$ for $\Upsilon(1S)$ , $\Upsilon(2S)$ , $\Upsilon(3S)$

The inclusive production cross section for  $\Upsilon$  mesons has been measured over the kinematic range  $|y^\Upsilon| < 0.4$  and  $0 < P_T^\Upsilon < 20 \text{ GeV}/c$ . We use a  $77 \text{ pb}^{-1}$  subset of the data, a significantly larger sample than in the previous published result.  $\Upsilon(1S)$ ,  $\Upsilon(2S)$

and  $\Upsilon(3S)$  candidates are counted by fitting the dimuon invariant mass distribution to Gaussian signals on a quadratic background. The acceptance and efficiency in each  $P_T$  bin are calculated using a simulation of the detector and trigger. The resulting cross sections are shown in Fig. 1. A comparison of the normalized  $\Upsilon(1S)$ ,  $\Upsilon(2S)$  and  $\Upsilon(3S)$  cross sections shows that they have similar shapes.

### 3. $\Upsilon(1S)$ production from $\chi_b$ feeddown

The production of  $\chi_b(1P)$  and  $\chi_b(2P)$  mesons has been observed by fully reconstructing their decays to  $\Upsilon(1S)+\gamma$ .  $\Upsilon(1S)$  candidates with  $P_T > 8$  GeV/ $c$  are combined with photons with  $E_T^\gamma > 0.7$  GeV/ $c$ . The  $\Upsilon(1S)$   $P_T$  requirement removes events with large backgrounds from low energy photons. The combined invariant mass distribution is shown in Fig. 2. Background to the  $\chi_b$  signal is primarily due to real photons from  $\pi^0$  and  $\eta$  decays. To model the shape of the background, a Monte Carlo method is used: real charged particles in each event are “replaced” by  $\pi^0$ ,  $\eta$  and  $K_S^0 \rightarrow \pi^0\pi^0$ . The photons obtained from these fake decays are passed through a detector simulation and combined with the real  $\Upsilon(1S)$  candidates. Clear  $\chi_b(1P)$  and  $\chi_b(2P)$  signals can be seen in Fig. 2, while no  $\chi_b(3P)$  signal is apparent. Taking into account the acceptance and efficiency for reconstructing the photons, we measure the fractions of  $\Upsilon(1S)$  with  $P_T > 8$  GeV/ $c$  produced by  $\chi_b(1P)$  and  $\chi_b(2P)$  decays to be  $(26.7 \pm 6.9 \pm 4.3)\%$  and  $(10.8 \pm 4.4 \pm 1.3)\%$  respectively. Then, subtracting the calculated fraction of  $\Upsilon(1S)$  produced by  $\Upsilon(2S, 3S)$  decays, we obtain the direct fraction of  $\Upsilon(1S)$  with  $P_T > 8$  GeV/ $c$ :  $(51.8 \pm 8.2 \pm_{6.7}^{9.0})\%$ .

### 4. $\Upsilon(1S)$ polarization

The production polarization of  $\Upsilon$  (and  $\psi$ ) mesons is measured using the distribution of the decay angle  $\theta^*$ . This is the angle between the  $\mu^+$  direction in the meson rest frame and the meson direction in the lab frame. The distribution has the form  $1 + \alpha \cos^2 \theta^*$ , where the polarization parameter  $\alpha$  is +1 in the case of transverse polarization, -1 for longitudinal and 0 for unpolarized production.

The  $\Upsilon(1S)$  polarization has been measured over the range  $|y^{\Upsilon(1S)}| < 0.4$ , by fitting the observed distribution of  $\cos \theta^*$  to a sum of transverse and longitudinal Monte Carlo templates. These templates are drawn from generated samples of

‡ Transverse energy  $E_T \equiv E \cdot \sin \theta$ , analogous to  $P_T$ .

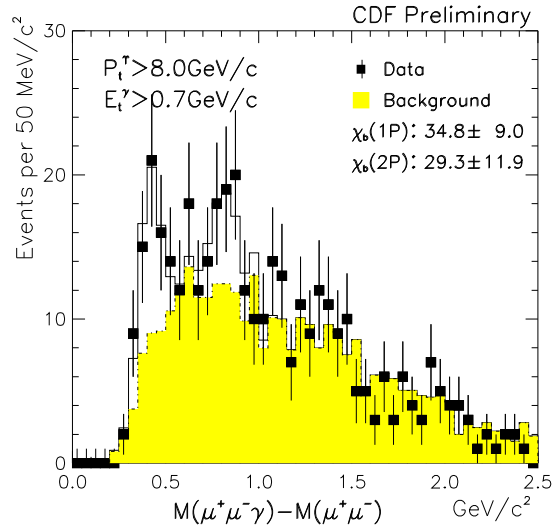


**Figure 2.**  $\Upsilon(1S)\gamma$  invariant mass distribution, showing  $\chi_b(1P)$  and  $\chi_b(2P)$  signals above background.

$\Upsilon(1S)$  decays with  $\alpha = +1$  (or  $-1$ ), which have been passed through detector and trigger simulations to account for the dependence of the acceptance on  $\cos \theta^*$ . Using a data sample of approximately 4,400  $\Upsilon(1S)$  decays, the fitted longitudinal fraction for the  $P_T$  range 2 – 20 GeV/ $c$  is  $\Gamma_L/\Gamma = 0.37 \pm 0.04$ , consistent with no polarization. In the more restricted  $P_T$  range of 8 – 20 GeV/ $c$ , the fitted fraction is  $\Gamma_L/\Gamma = 0.32 \pm 0.11$ . These values represent the inclusive  $\Upsilon(1S)$  polarization, as it is not possible to separate direct production from feeddown in this measurement.

Measuring the production polarization has also significantly reduced the systematic uncertainty on the cross section measurement of section 2.

### 5. Prompt $J/\psi$ polarization

The  $J/\psi$  polarization has been measured over the kinematic range  $|y^{J/\psi}| < 0.6$ , using approximately 180,000  $J/\psi$  decays. The polarization is measured both for promptly produced  $J/\psi$  mesons and for those produced in  $B$ -hadron decays. The values of  $\alpha_{Prompt}$  and  $\alpha_B$  are measured in seven  $P_T$  bins, covering 4 – 20 GeV/ $c$ . As with the  $\Upsilon(1S)$ , it is not feasible to separate the feeddown (from  $\chi_c$  and  $\psi(2S)$  decays), which accounts for about 35% of the prompt component [3].

The precise vertex tracking done by the SVX is used to separate the prompt and  $B$ -decay components. The two muon tracks are fitted

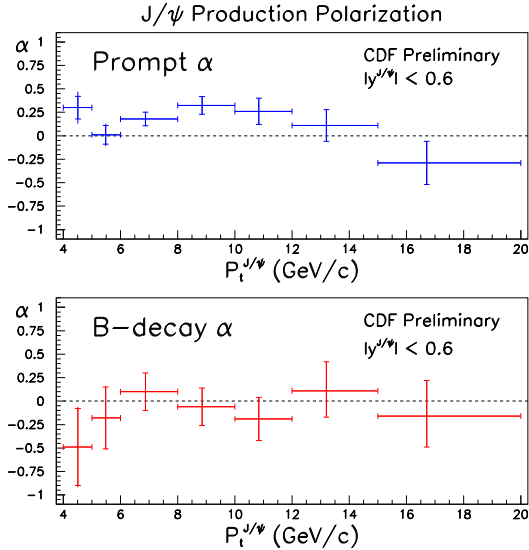


**Figure 3.** The polarization parameter  $\alpha$  as a function of  $P_T$ , for prompt  $J/\psi$  mesons and for  $J/\psi$  mesons from  $B$ -hadron decay.

to a common vertex, and the displacement of this vertex from the beamline is converted into an estimate of  $ct$ , the proper lifetime of the decay. Prompt  $J/\psi$  candidates have  $ct$  consistent with zero, whereas those from  $B$  decay have an exponential  $ct$  distribution.  $J/\psi$  candidates are divided into short-lived and long-lived samples based on their  $ct$ . These two samples are dominated by prompt production and  $B$ -decay respectively, and the actual fractions of prompt and  $B$ -decay in each are measured using a maximum-likelihood lifetime fit.

The polarization fit, as in the  $\Upsilon(1S)$  case, uses Monte Carlo templates to account for the detector and trigger acceptance. The  $\cos\theta^*$  distributions in the short- and long-lived samples are simultaneously fitted for  $\alpha_{Prompt}$  and  $\alpha_B$ . A third sample, in which the muons do not have SVX information, is also included in the fit to improve the overall precision on  $\alpha$ . The fit results are shown in Fig. 3. The prompt polarization does not display a significant increase at high  $P_T$ . Although  $\alpha_{Prompt}$  includes contribution from feeddown, this result does not seem to support predictions of predominantly transverse polarization given in [6].

## 6. Prompt $\psi(2S)$ polarization

The procedure for measuring prompt  $\psi(2S)$  polarization is largely similar to that in the  $J/\psi$  case. However, this measurement is more

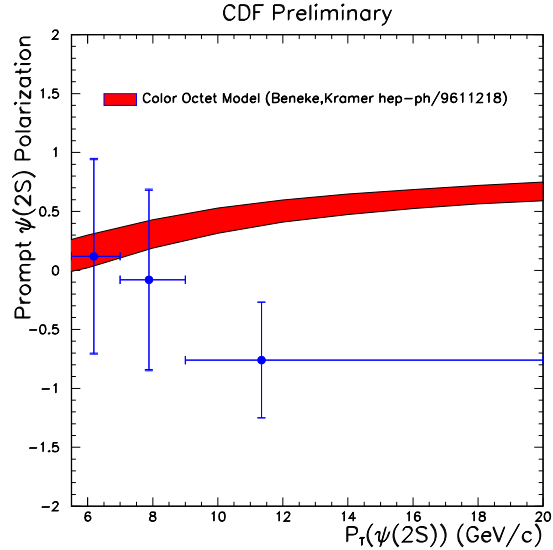


**Figure 4.** The polarization parameter  $\alpha$  as a function of  $P_T$  for prompt  $\psi(2S)$  mesons, compared to a color octet model prediction.

statistically limited, as there are about 1,800  $\psi(2S) \rightarrow \mu^+\mu^-$  candidates. Since the  $\psi(2S)$  incurs no feeddown from heavier  $c\bar{c}$  states, the prompt polarization (shown in Fig. 4) is equivalent to the direct polarization. At high  $P_T$ , our measurement does not appear to support the model's prediction.

## 7. Summary

We have presented recent measurements of  $\Upsilon$  cross sections,  $\chi_b \rightarrow \Upsilon(1S)$  feeddown, and  $\Upsilon(1S)$ ,  $J/\psi$  and  $\psi(2S)$  polarization. We look forward to the use of this information in quarkonium production models.

## References

- [1] F. Abe *et al.* (The CDF Collaboration), *Phys. Rev. Lett.* **79**, 572 (1997).
- [2] F. Abe *et al.* (The CDF Collaboration), *Phys. Rev. Lett.* **75**, 4358 (1995).
- [3] F. Abe *et al.* (The CDF Collaboration), *Phys. Rev. Lett.* **79**, 578 (1997).
- [4] E. Glover, A. Martin & W. Stirling, *Z. Phys. C* **38**, 473 (1988).
- [5] P. Cho & A. Leibovich, *Phys. Rev. D* **53**, 6203 (1996); E. Braaten & S. Fleming, *Phys. Rev. Lett.* **74**, 3327 (1995).
- [6] P. Cho & M. Wise, *Phys. Lett. B* **346**, 129 (1995); M. Beneke & M. Krämer, *Phys. Rev. D* **55**, 5269 (1997).